Title
ELEVATED TEMPERATURE DEFORMATION MECHANISMS IN -NiAl

Authors
Vandervoort, R.R.
Mukherjee, A.K.
Dorn, J.E.

Publication Date
1966-05-01

UCRL-16388

University of California

Ernest O. Lawrence Radiation Laboratory

ELEVATED TEMPERATURE DEFORMATION MECHANISMS IN β'-NiAl

Berkeley, California

DISCLAIMER

Submitted to Amer. Society
for Metals

UCRL-16388

UNIVERSITY OF CALIFORNIA

Lawrence Radiation Laboratory
Berkeley, California

AEC Contract Co. W-7405-eng-48

ELEVATED TEMPERATURE DEFORMATION MECHANISMS IN β'-NiAl

R. R. Vandervoort,[1] A. K. Mukherjee[2] and J. E. Dorn[3]

May, 1966

[1]Research Metallurgist, Lawrence Radiation Laboratory, University of California at Livermore.

[2]Currently Senior Scientist, Metal Science Group, Battelle Memorial Institute, Columbus.

[3]Professor of Materials Science of the Department of Mineral Technology, College of Engineering and Research Metallurgist of the Inorganic Materials Research Division of the Lawrence Radiation Laboratory, University of California, Berkeley.

ABSTRACT

Polycrystalline specimens of the ordered intermetallic compound β'-NiAl were tested in compression in the temperature range 800° C to 1475° C. Three compositions were studied, namely 46.0, 49.6 and 56.0 at .% Ni. The effects of temperature, composition and strain rate on the flow stress were investigated. The rate controlling dislocation mechanisms are discussed. It was observed that the high temperature deformation of the alloys appeared to be controlled by a viscous glide process, whereas the lower temperature deformation of the 49.6 and 56.0 at .% Ni alloys was governed by a new, as yet unidentified, mechanism.

ordered structure (CsCl type) up to its melting point of 1638° C. Therefore, it was possible to study the deformation characteristics of an ordered alloy over a wide temperature range above 1/2 T_m where diffusion is expected to play an important role in the deformation process. Second, NiAl has an ordered structure over a range of composition. Deviations from the equiatomic composition produce very interesting defect structures. Excess nickel atoms substitute for aluminum atoms, but excess aluminum atoms cannot replace the smaller nickel atoms and therefore some nickel lattice sites are left vacant.[9,10] Consequently, study of the deformation of nonstoichiometric alloys may permit an evaluation of the influence of substitutional atoms or excess lattice vacancies on the creep of NiAl.

II. EXPERIMENTAL PROCEDURE

The starting materials for casting the NiAl ingots were 99.99% Ni and 99.999% Al. The melting was done in an induction furnace using purified argon gas and a water cooled copper boat. This casting technique[11] produced irregularly shaped cylindrical ingots about 5 in. in length and 1/2 in. in diameter. Three compositions were prepared having chemical analyses of 49.6 ± 0.2, 46.0 ± 0.3 and 56.0 ± 0.3 atomic percent nickel, respectively. Typical impurity levels in p.p.m. were as follows, Fe 100, Cu 30, Mg 3. No other metallic impurities were detected.

Considerable difficulty was encountered in preparing test specimens from the ingots because of extreme brittleness of these alloys at room temperature. Conventional grinding and machining methods were abandoned as a result of the inability to obtain specimens free from surface chips.

It was found, however, that a spark-erosion process produced crack-free and essentially strain-free specimens.[12] After turning and sectioning the ingots, the ends of the cylinders were lapped parallel to within ±1.5 mils by standard metallographic techniques. Final diameters of the test specimens ranged between 0.375 in. and 0.400 in. The height of all specimens was about 0.5 in.

Specimens were tested in compression in an Instron testing machine. The signal from the load cell in association with a recording instrument provided a continuous load-time plot. Changes in cross-head velocity were made by a gear shift arrangement.

The furnace was heated by semi-cylindrical tantalum sheet elements. The elements were surrounded by five layers of heat shields. The furnace hot zone was 6 in. long and there was no detectable gradient in the central 1 in. The specimens were compressed between aluminum oxide rams. Tests were conducted in vacuum in the temperature range 800° to 1475° C. The temperature was measured by a Pt- Pt 10% Rh thermocouple and was controlled within ±2° C of the reported values.

III. EXPERIMENTAL RESULTS

The central portion of the NiAl phase diagram had been established by x-ray diffraction of powders slowly cooled from 800° C[9] and by thermal arrest and micrographic analyses.[13] Although these studies indicate that alloys near the equiatomic composition remain ordered up to the melting point, it has also been reported that NiAl disorders at elevated temperatures.[14] Because this investigation was undertaken to study the deformation characteristics of a long-range ordered alloy it was deemed necessary to verify the existence of the ordered structure

in the temperature region 800 to 1475° C. To accomplish this purpose x-ray diffraction photographs of powdered NiAl samples were taken in a high temperature x-ray camera. Superlattice lines were observed in every pattern up to 1350° C which was the maximum temperature attainable by the equipment. There was no detectable decrease in the intensity with increasing temperature of the (210) superlattice diffraction line in relation to the (211) diffraction line.

When a material disorders its strength decreases abruptly,[1-5] but no discontinuity occurred in the present data between 1350° and 1475° C. This fact plus the high temperature x-ray diffraction results up to 1350° C make it almost certain that the NiAl alloy remains ordered over the entire range of test temperatures.

Metallographic examination of the cast ingots showed that the alloy was single phase. The grains were coarse but equiaxed. The grain size of the three alloys was determined by use of Jeffries' planimetric method. There were respectively 3 grains per square millimeter for the high aluminum and high nickel alloys and 1 grain per square millimeter for the equiatomic alloy.

The load-time record obtained from a compression test, in conjunction with the cross-head velocity, chart speed, and specimen dimensions was converted into a true stress-strain curve. An example of the deformation behavior of NiAl at constant temperature is illustrated in Fig. 1. This curve is typical of that obtained on all three alloys. The transients occurring at each strain rate before steady state is achieved indicate that some type of structural change is taking place. The total deformation calculated using the load-time

chart agreed with that measured directly from the specimens after testing. It should be pointed out that specimens tested at constant deformation rate and constant temperature showed no significant work hardening up to a strain of 15% following the small initial transient stage. Lautenschlager et al. reported that ordered NiAl alloys exhibited serrated stress-strain curves,[15] but no such effect was detected in the present work. Significant rates of strain hardening were also observed by Lautenschlager and his coworkers. Oxygen contamination has been shown to increase the hardness of intermetallic compounds near grain boundaries,[16,17] and, perhaps, the differences in stress-strain curves may be the result of impurity effects. Comparison of flow stress at constant temperature reveals that the alloys tested in this work are weaker than those in the former investigation. This lends support to the supposition that the impurity content in the present alloys may have been lower.

The steady-state flow stress at five strain rates for the three alloys is plotted as a function of temperature in Figs. 2a, 2b and 2c. The shear stress was taken to be one-half of the compressive stress, and the shear strain rate was taken as three-fourths of the compressive strain rate. These data clearly show that the deformation process is thermally activated. This result, however, is not unexpected as it has been well documented that slow deformation at temperatures in excess of one-half the absolute melting temperature is usually controlled by diffusion processes.[18]

The effect of the shear stress τ on the creep rate $\dot{\gamma}$ at constant temperature for the high aluminum alloy is illustrated in Fig. 3.

Approximately a linear relationship exists between log $\dot{\gamma}$ and log τ over the range of strain rates and stress studied, and the lines have nearly constant slope for all temperatures. These data reveal that the equation

$$\dot{\gamma} \propto \tau^{3.4 \pm 0.2} \qquad (1)$$

can describe the stress law for this alloy.

The strain rate dependence on stress for the equatomic alloy is portrayed in Fig. 4. The curves on the log $\dot{\gamma}$ versus log τ graph are linear, but as can be seen, the slope of the lines decreases as the test temperature increases. This suggests that the apparent activation energy for deformation is not constant but is some function of the stress except possibly for the lowest stresses.

The curves on the log γ - log τ plot for the high nickel alloy can be divided in two groups (Fig. 5). The lines for temperatures of 1100°C and higher are nearly parallel and the following power law relation represents these results:

$$\dot{\gamma} \alpha \tau^{3.7 \pm 0.1} \qquad (2)$$

At 1025°C and below the slope of the lines increases as the temperature decreases, indicating that the activation energy depends on stress in this temperature region. The high temperature behavior of the high nickel alloy is similar to the deformation behavior of the high aluminum alloy while at lower temperatures its deformation characteristics resemble those of the stoichiometric alloy.

The apparent activation energies, Q, for deformation, as recorded in Fig. 6, were deduced from the data given in Figs. 3, 4 and 5 using the well known definition

$$Q = \frac{\Delta \ell n \dot{\gamma}}{\Delta(-\frac{1}{RT})}_{\tau} \qquad (3)$$

Whereas the apparent activation energy was found to have a constant value of 65,000 cal/mole independent of stress for the 46.0 at.% Ni alloy, that for the 56.0 at.% Ni alloys appeared to exhibit two regions. For the lower stress (or high temperature) region the activation energy had a constant value of about 78,000 cal/mole while for the higher stresses (or lower temperatures) the apparent activation energy was sensitive to the stress and decreased very nearly linearly with the logarithm of the stress. The 49.6 at.% Ni alloy also exhibited a high stress (or low temperature) region where the activation energy decreased linearly with the logarithm of the stress, and appeared to have a low stress (or high temperature region having a constant activation energy of about 69,000 cal/mole. Although the τ-T curves of Figs. 2a, 2b and 2c do not readily reveal the existence of the two types of behavior, their presence is easily seen by the data recorded in Figs. 3 to 6. Obviously at least two different dislocation mechanisms (a high temperature and a low temperature mechanism) are operative in these alloys. Furthermore, the temperature of inception of these mechanisms is dependent on composition.

IV. DISCUSSION

A. Modes of Deformation

Several long-range ordered alloys having the CsCl type of lattice are known to glide by motion of pairs of a/2 $\langle 111 \rangle$ superpartial dislocations on planes of the form {110}, {112}, and (or) {123}. An

early slip trace analysis on polycrystals by Westbrook[17] suggested that slip in NiAl takes place on the {123} planes by motion of the a/2 ⟨111⟩ superpartial dislocations. If this were so, high-temperature deformation of NiAl would have been dependent on recovery of antiphase boundaries produced by viscous creep or by the formation of antiphase boundary tubes as reviewed recently by Dorn and Mitchell.[19] Analyses of the data presented here, however, were in disagreement with these possible mechanisms. More recently, however, Rozner and Wasilewski,[20] reported that single crystals of NiAl glide on the {100} and {110} planes by motion of the total a⟨001⟩ dislocations. The existence of a defect lattice for the high Al composition and the observed modes of slip are consistent since they indicate the presence of some degree of ionic bonding in NiAl.

B. High Temperature Deformation

As previously discussed, the apparent activation energy for deformation of the NiAl alloys investigated was a constant independent of the stress in the high temperature range. This observation disqualifies such mechanisms as intersection, Peierls, cross slip and motion of jogged screw dislocations etc. for which the activation energy is a function of the stress. The two most likely known mechanisms thus reduce to either the climb of dislocations[21] or the viscous flow mechanism.[22] The former, however, usually exhibits a strain rate that increases with the stress to about the fifth power whereas the current experimental data show that $\dot{\gamma} \propto \tau^{3.3}$ in the range under question. This suggests, therefore, that Weertman's viscous creep mechanism is the most likely process. As described by Dorn and Mitchell,[23] for diffusion controlled

viscous creep by Weertman's model,

$$\dot{\gamma} = \frac{2\pi(1-\mu)\ \tau^3 b^3\ Nz\ v}{RTG^2}\ e^{\frac{\Delta S}{R}}\ e^{\frac{\Delta H}{RT}} \qquad (4)$$

where μ = Poisson's ratio, b = Burgers' vector, N = Avogadro's number, z = coordination number, v = Debye frequency, R = gas constant, T = absolute temperature, G = shear modulus of elasticity and ΔS and ΔH are the entropy and enthalpy of activation. While experimental data show that $\dot{\gamma} \propto \tau^{3.3}$ to $\tau^{3.6}$ Weertman's model predicts that $\dot{\gamma} \propto \tau^3$. In view of the approximations made in the theoretical model, this discrepancy is not excessive.

In short-range ordered alloys ΔS is the average entropy for diffusion and ΔH is equal to some average enthalpy for diffusion plus the disordering energy. For the NiAl lattice, however, when slip occurs by the perfect Burgers' vector b = a[001] the exact meanings of ΔS and ΔH are uncertain because the diffusion processes in such ordered alloys have not yet been clearly established. At least two activation energies for diffusion will eventually have to be appropriately incorporated into the analysis. In the absence of such detailed knowledge, however, it will be assumed here that the ΔH is some average value for the atomic species on the two lattice sites. The apparent activation energy for this approximation becomes

$$Q = \frac{\partial \ell n \dot{\gamma}}{\partial(-\frac{1}{RT})} = \Delta H + \frac{\partial \ell n(TG^2)}{\partial(\frac{1}{RT})}$$

Although the data required to obtain the last term are not yet known, it seldom exceeds about 2,000 to 3,000 cal/mole. Consequently $\Delta H \simeq Q$.

The only known data permitting a comparison is that obtained by Berkowitz, Jaumot and Nix for the diffusion of Co^{60} in NiAl alloys.[24] (Fig. 7). (The diffusion data for the highest Ni alloy were uncertain. Reanalysis of these data indicates that the activation energy should have been at the suggested position in the graph.) Because of their similarities it is expected that the activation energy for diffusion of Ni in pure NiAl alloys cannot differ much from that for Co^{60}. The apparent activation energies for creep, obtained here, are also recorded on the same graph. In view of the fact that the 46.0 at.% Ni alloy forms a defect lattice it is expected to have the lowest value of the activation energy for creep; the slightly higher activation energies obtained for creep than those reported for diffusion of Co in the NiAl alloys are qualitatively expected.

The experimental deformation data at high temperatures for each of the alloys can be summarized by $\dot{\gamma} \simeq A\, \tau^n\, e^{-\frac{\Delta H}{RT}}$ as given in Table I.

Table I

alloy at.% Ni	ΔH cal/mole	n_{exp}	n_{theory}	$\dot{\gamma}_{exp}$	$\dot{\gamma}_{theory}$
46.0	65,000	3.3	3.0	3.6×10^{-4}	5.1×10^{-4}
49.6	~69,000	3.3	3.0	1.5×10^{-4}	1.1×10^{-4}
56.0	78,000	3.7	3.0	1.9×10^{-4}	3.9×10^{-5}

The last column gives the values of $\dot{\gamma}$ estimated from Eq. (4) by taking

$$\mu = 0.3 \qquad b = 2.9\text{Å} \qquad G = 1.1 \times 10^{12} \frac{\text{dynes}}{\text{cm}^2}$$

$$T = 1500^\circ\text{K} \qquad z = 8 \qquad \nu = 10^{13}\,1/\text{sec}$$

$$\Delta S/R = 1 \qquad N = 6.02 \times 10^{23} \qquad R = 2.0 \frac{\text{cal}}{\text{mole}}\,{}^\circ\text{K} \qquad \tau = 750 \text{ psi}$$

In view of the simplifications and gross averaging methods adopted in the theory, the agreement between the experimental and theoretical values of $\dot{\gamma}$ is as good as can be expected.

C. Intermediate Temperature Deformation

All three alloys appeared to deform in nominal accord with Weertman's viscous flow mechanism at the higher temperatures. Although the defect lattice of the 46.0 at.% Ni alloy continued to exhibit this mechanism over the entire range of temperatures that were studied, both the 49.6 and 56.0 at.% Ni alloys showed a transition to a new mechanism (vide Fig. 6), characterized by an activation energy that decreased almost linearly with $\ell n\ \tau$ over the intermediate temperature range. Since efforts to correlate these data with such mechanisms as the Peierls process, intersection and motion of jogged screw dislocations for which the activation energy is sensitive to the stress failed to yield agreement, it appears that some as yet unidentified mechanism applies.

Although the details of the mechanism are not known it is possible to suggest a semi-empirical formulation which any adequate model must eventually confirm. We assume that the deformation arises from a single mechanism of thermally activated dislocation motion over barriers. Therefore, the strain rate is given by the usual expression of

$$\dot{\gamma} = (\rho/L)(L^2)b\ \nu' \tag{5}$$

where ρ is the density of the mobile dislocations, ρ/L the number of dislocation segments held up at barriers per unit volume (L being the mean distance between barriers). L^2 is the volume swept out per activation and ν' is the frequency of activation. To a good approximation,

$$\nu' = \frac{\nu\ b\ e^{-U/kT}}{L} \tag{6}$$

where ν is the Debye frequency and U is the activation energy. Consequently the strain rate is given by

$$\dot{\gamma} = \rho b^2 \nu e^{-U/kT} \tag{7}$$

The experimental data reveal that the activation energy is given by

$$U = m(\ell n\ \tau_o - \ell n\ \tau) \tag{8}$$

where m and τ_o are substantially constants for each alloy. (The possible effect of the variation of shear modulus of elasticity with temperature on these constants is minor and will be neglected here.) The activation volumes, defined by

$$v^* = -\frac{\partial U}{\partial \tau} = \frac{m}{\tau} \tag{9}$$

are shown in Fig. 8 in terms of v^*/b^3, versus τ and are noted to be within permissible ranges for thermally activated dislocation mechanisms. Eqs. (7) and (8) give

$$\ell n\ \dot{\gamma} = \ell n\ \rho + \ell n\ b^2 v + \frac{m}{kT}\ \ell n \tau - \frac{m}{kT}\ \ell n\ \tau o \tag{10}$$

But the experimentally determined variation of $\ell n\ \dot{\gamma}$ with $\ell n\ \tau$ has a greater slope than m/kT, suggesting, in agreement with other observations on high temperature creep,[25] that the density of mobile dislocation, ρ, also increases with the stress. The variation of ρ with stress was

deduced from Eq. (7), using the experimentally determined activation energies and strain rates employing $b = 2.9 \times 10^{-8}$ cm and $\nu = 10^{13}$ per second. As shown in Fig. 9, the values of ρ correlate quite well with τ regardless of the test temperature or strain rate. While the estimated densities of the mobile dislocations for the 56.0 atomic % Ni alloy appear to be slightly high, those for the 49.6 atomic percent Ni alloy fall in the expected range.

One of the several objectives of this investigation was concerned with the effect of excess vacancies in the defect lattice of the 46. at.% Ni alloy and the effect of excess substitutional Ni in the 56.0 at.% Ni alloy in modifying the deformation characteristics of the almost stoichiometric alloy containing 49.6 at.% Ni. The effects of temperature on the flow stresses of these alloys for a shear strain rate of 10^{-4} per sec are shown in Fig. 10. These trends are in nominal agreement with previously reported hardness versus composition isotherms for AgMg.[26] The trends also agree well with the hardness data on NiAl reported by Westbrook[27] and are in nominal agreement with the compression test data of Lautenschlager.[15] Previous discussions in the literature on the effect of composition on the behavior of NiAl alloys are somewhat questionable because effects of transitions in mechanisms were not considered. The ranges of operation of the two mechanisms isolated in this study are recorded in Fig. 10. At 1250°C and above all three alloys deform by the diffusion controlled viscous creep mechanism. The fact that the flow stress is least for the 46.0 and greatest for the 49.6 at.% Ni alloy is wholly consistent with the known trends on the variation of diffusivities[24, 28-30] with composition in ordered alloys.

Whereas the 49.6 and the 56.0 at.% Ni alloys exhibit a change in mechanism as the temperature is reduced to below about 1200°C, it is not surprising that the 46.0 at.% Ni alloy continues to undertake viscous creep at yet lower temperatures because of the large vacancy concentration in the defect lattice of this alloy.

Since the operative mechanism for deformation of the 49.6 and 56.0 at.% Ni alloy below 1200°C has not been identified, the factors responsible for the higher flow stress of the higher Ni content alloy cannot, as yet, be rationalized.

SUMMARY AND CONCLUSIONS

1. The compression properties of cast polycrystalline β'-NiAl containing 46.0, 49.6, and 56.0 atomic percent Ni, respectively, were determined over the range of temperatures from 800° to 1475°C and over a range of strain rates from 1.2×10^{-5} to 1.3×10^{-3} per second.

2. Determination of the apparent activation energies and effect of stress on the strain rate revealed that the alloys undertook two distinctly different mechanisms of deformation as follows:

Suggested Mechanism	Alloy At % Ni	Range °C	Activation Energy cal/mole	n
Viscous	46.0	1400-800	64,500	3.3
motion of	49.6	1400-1250	69,500	3.5
dislocations	56.0	1400-1175	78,000	3.7
	46.0	Not observed		
New	49.5	1250-800	Decreasing linearly with ln(stress)	
Mechanism	56.0	1175-800		

3. The activation energies for the viscous mechanism were independent of the stress and approximated those estimated for diffusion. The strain rate for the viscous mechanism was given by $\dot{\gamma} \propto \tau^n$ where n, shown above, was only slightly greater than that of 3 suggested by Weertman's theory.

4. For the unidentified new mechanism the activation energy decreased linearly with the logarithum of the stress and the strain-rate increased with a power of the stress that increased as the temperature was decreased. An attempt was made to present a semi-theoretical description of the new mechanism.

ACKNOWLEDGEMENT

This report was prepared as part of the activities of the Inorganic Materials Research Division of the Lawrence Radiation Laboratory, University of California, Berkeley, and was done under the auspices of the United States Atomic Energy Commission.

REFERENCES

1. M. Herman and N. Brown, Trans. AIME, (1956), 206, 604.
2. A. Lawley, J. Coll, and R. Cahn, (1960), 218, 166.
3. T. Suzuki and M. Yamamoto, J. Phys. Soc. Japan, (1959), 14, 463.
4. R. Davies, Trans, AIME, (1963), 227, 277.
5. A. Soler-Gomez and W. McG. Tegart, Acta Met., (1964), 12, 961.
6. E. Howard, W. Barmore, J. Mote, and J. Dorn, Trans. AIME, (1963), 227, 1061.
7. R. Wakelin and E. Yates, Proc. Phys. Soc., (London) (1953), B66, 221.
8. A. Mukherjee and J. Dorn, J. Inst. Met., (1965), 94, 397.
9. A. Bradley and A. Taylor, Proc. Roy. Soc., (1937), [A], 159, 56.
10. M. Cooper, Phil. Mag., (1963), 8, 805.
11. H. Sterling and R. Warren, Metallurgia, (1963), 67, 1.
12. A. Szirmae and R. Fisher, Techniques of Electron Microscopy, Diffraction, and Microprobe Analysis, June 26, 1963, p. 1, A.S.T.M. Special Technical Publication No. 372.
13. W. Alexander and N. Vaughan, Proc. Roy. Soc., (1937), 61, 247.
14. I. Isaichev and V. Miretskii, Z. Tehk. Fiz. SSSR, (1940), 10, 316, Reported in Handbook of Lattice Spacings and Structures of Metals, W. Pearson, Pergamon Press, London (1958), 1044p.
15. E. Lautenschlager, D. Kiewit, and J. Brittain, Trans. AIME, (1965), 233, 1297.
16. J. Westbrook and D. Wood, J. Inst. Met., (1962), 91, 174.
17. A. Seybolt and J. Westbrook, Aeronautical Systems Division Report ASD-TDR-63-309, Part II, 38pp, April, 1964.

18. J. Dorn, Creep and Recovery, Seminar of the Am. Soc. Metals, Cleveland (1957) pp. 255-283.

19. J. Dorn and J. Mitchell, "Mechanisms of Creep in Ordered Alloys", UCRL 16562 Dec. 1965 (to be published in "Recent Progress in Applied Mechanics".)

20. A. G. Rogner and R. J. Wasilewski, J. Inst. Met. (1966) 94 169.

21. J. Weertman, J. Appl. Phys., (1955), 26, 1213.

22. J. Weertman, J. Appl. Phys., (1957), 28, 1185.

23. J. Dorn and J. Mitchell, "High-Strength Materials", John Wiley and Sons (1964) p. 510-577.

24. A. Berkowitz, F. Jaumot and F. Nix, Phys. Rev., (1954), 95, 1185.

25. J. E. Dorn and J. Mote, "High Temperature Structures and Materials" Pergamon Press (1963) p. 95-168.

26. J. Westbrook, J. Electrochem. Soc., (1957), 104, 369.

27. J. Westbrook, J. Electrochem. Soc., (1956), 103, 54.

28. F. Nix andF. Jaumot, Phys., Rev., (1951), 83, 1275.

29. W. Hagel and J. Westbrook, Trans. AIME, (1961), 221, 951.

30. H. Domian and H. Aaronson, Trans. AIME, (1964), 230, 44.

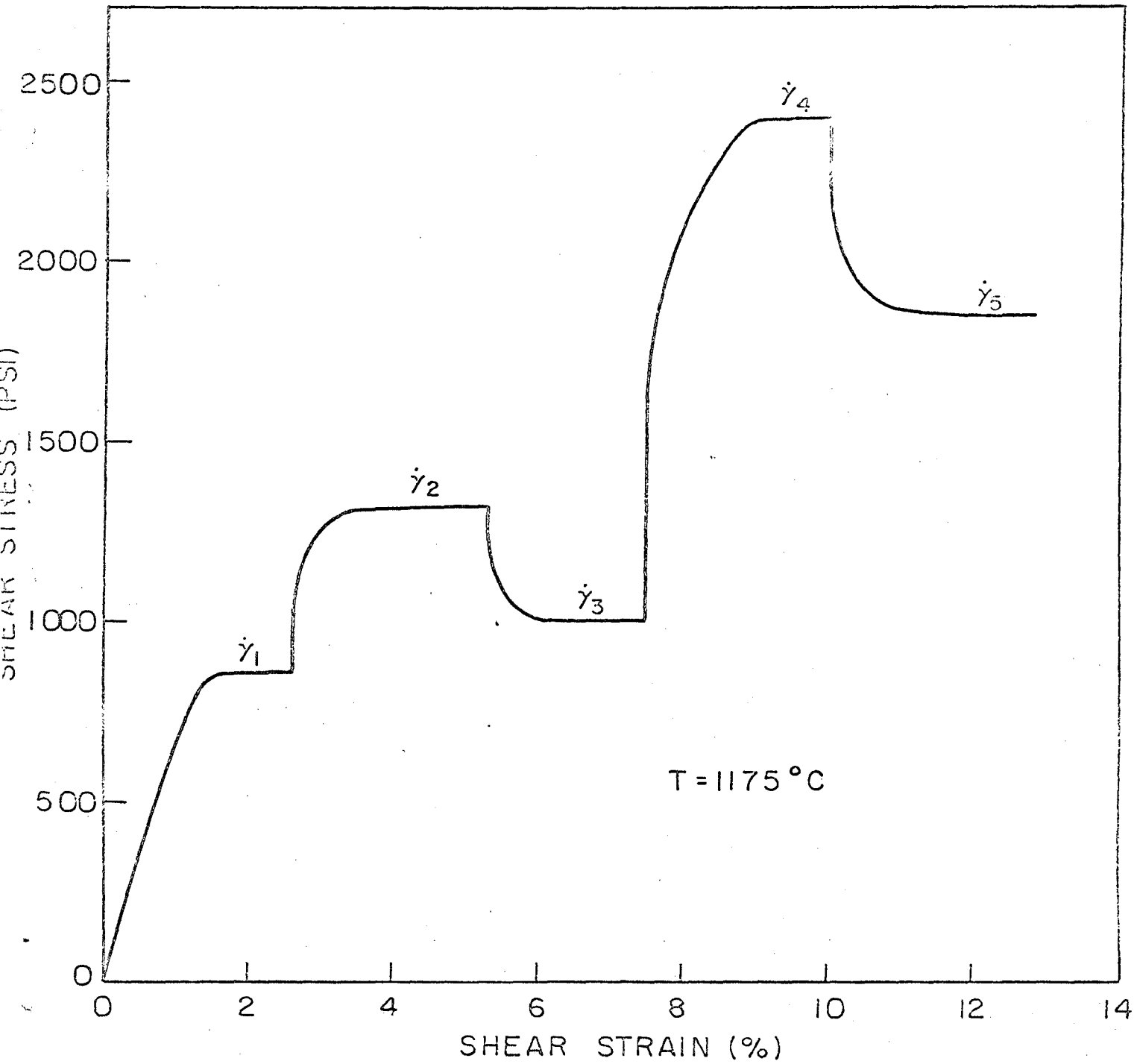

FIG. 1 FLOW SHEAR STRESS OBTAINED FOR FIVE DIFFERENT STRAIN RATES AT CONSTANT TEMPERATURES.

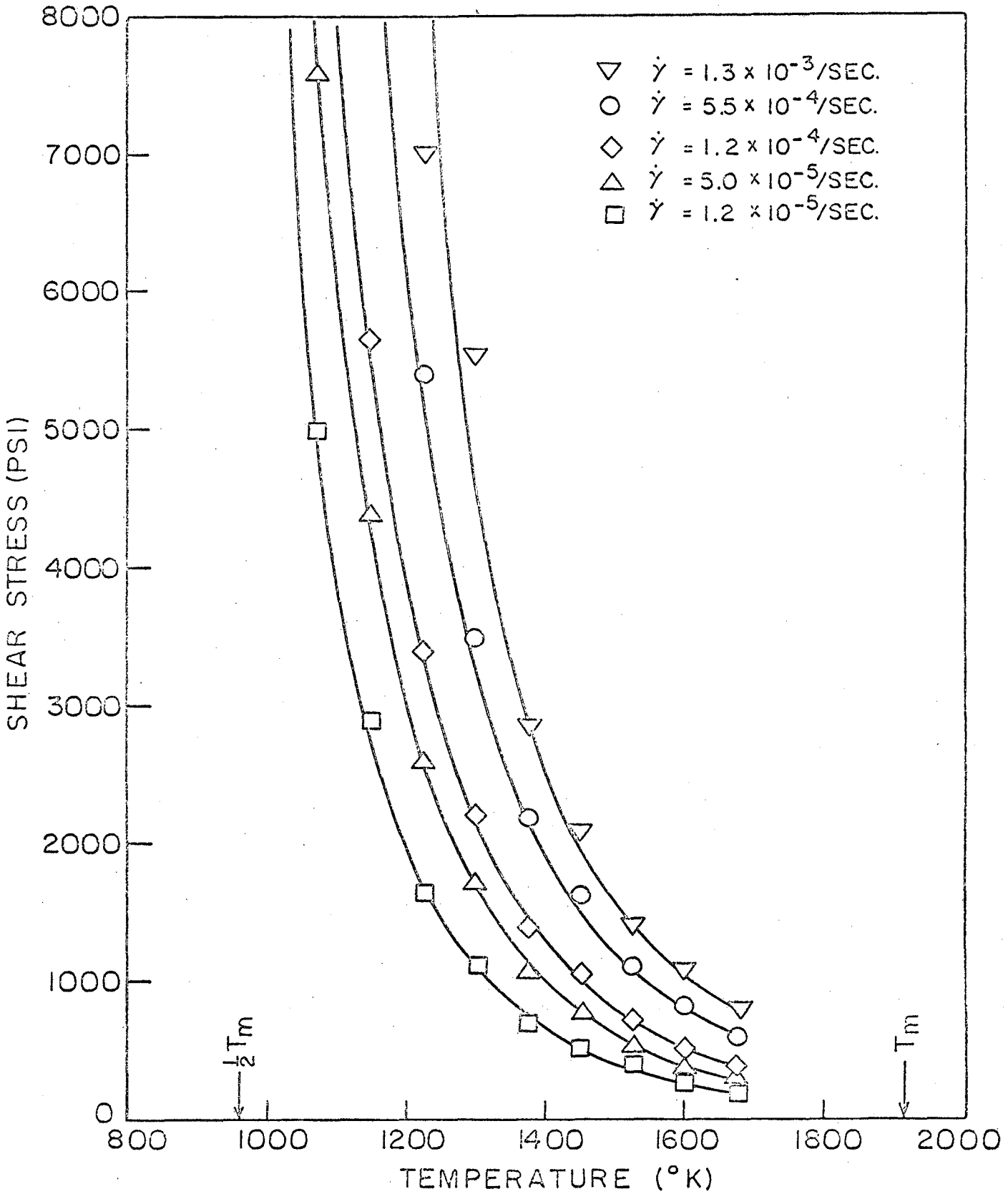

FIG. 2 A FLOW STRESS VERSUS TEMPERATURE FOR 46.0 AT. % NICKEL ALLOY.

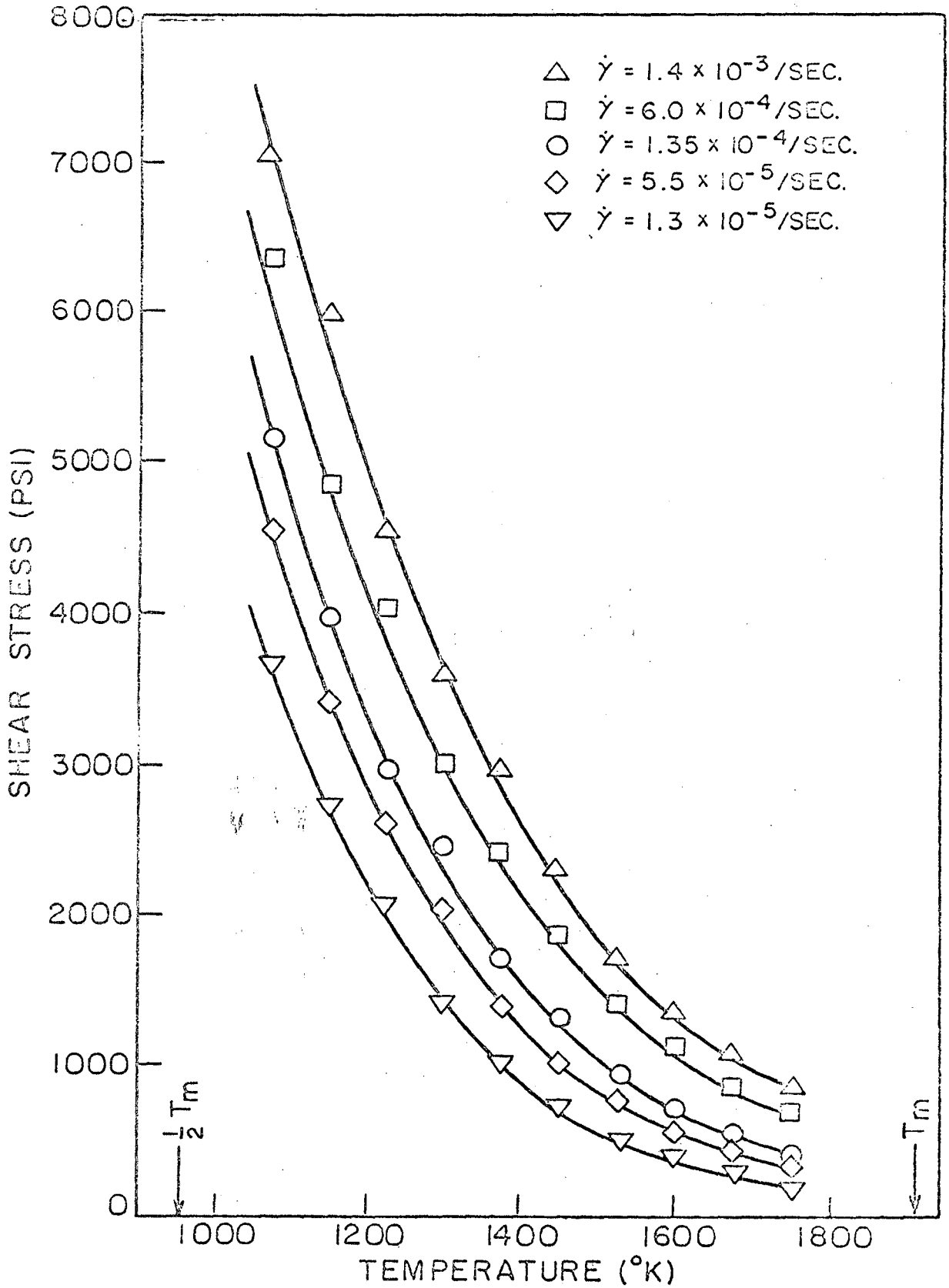

FIG. 2B FLOW STRESS VERSUS TEMPERATURE FOR 49.6 AT. % NICKEL ALLOY.

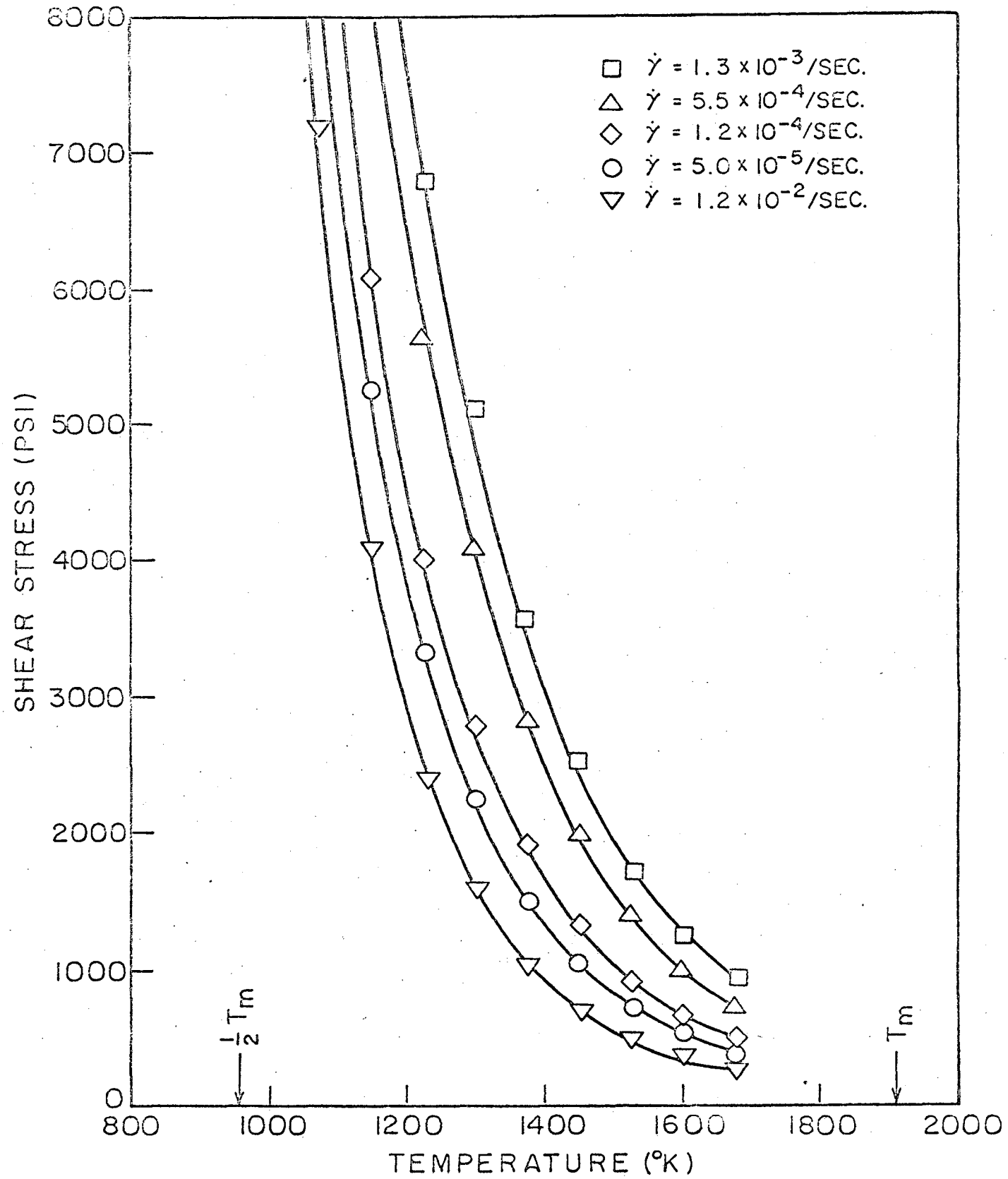

FIG. 2C. FLOW STRESS VERSUS TEMPERATURE FOR 56.0 AT. % NICKEL ALLOY.

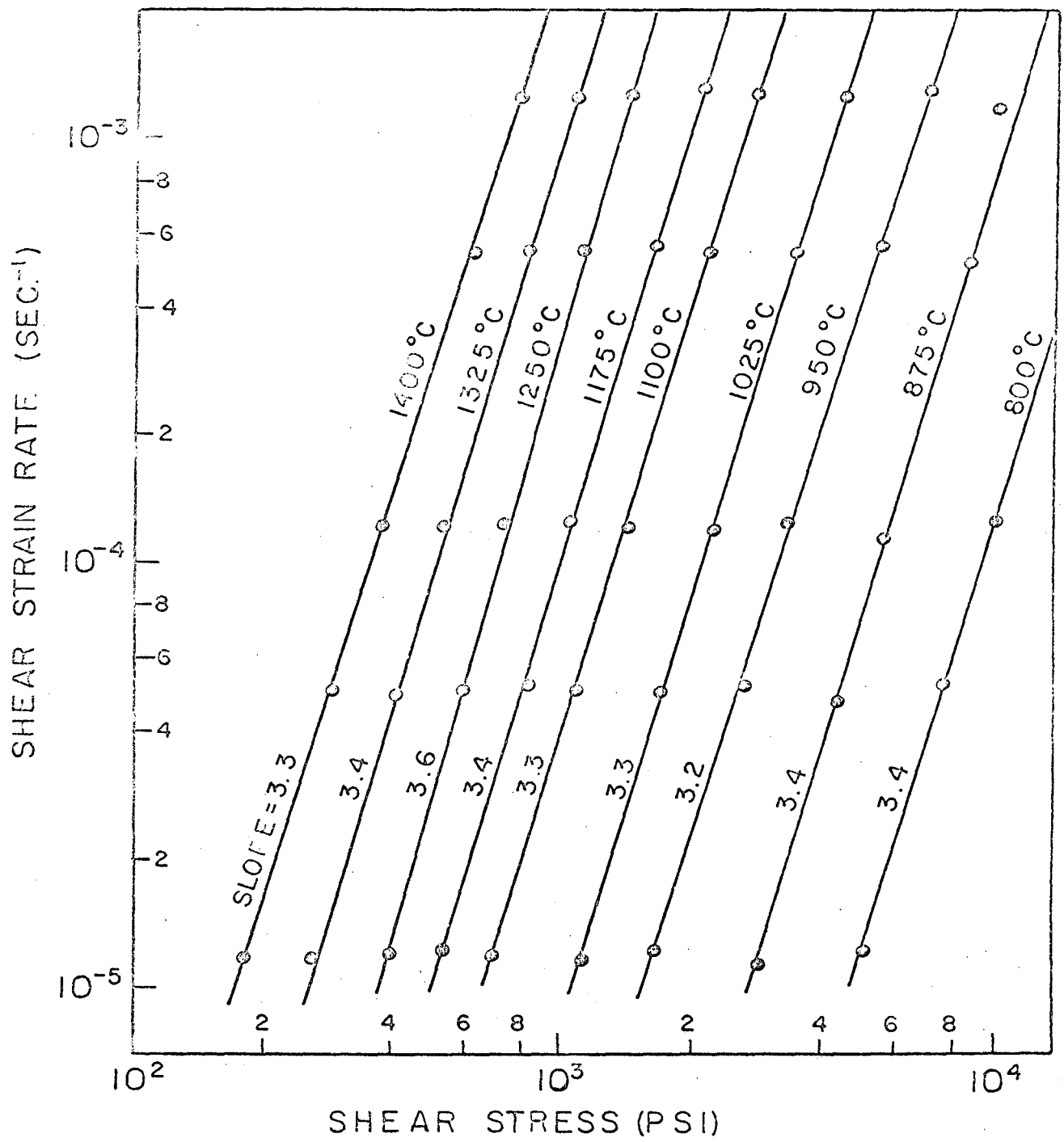

FIG. 3 EFFECT OF STRESS ON THE STRAIN RATE FOR 46.0 AT. % NICKEL ALLOY.

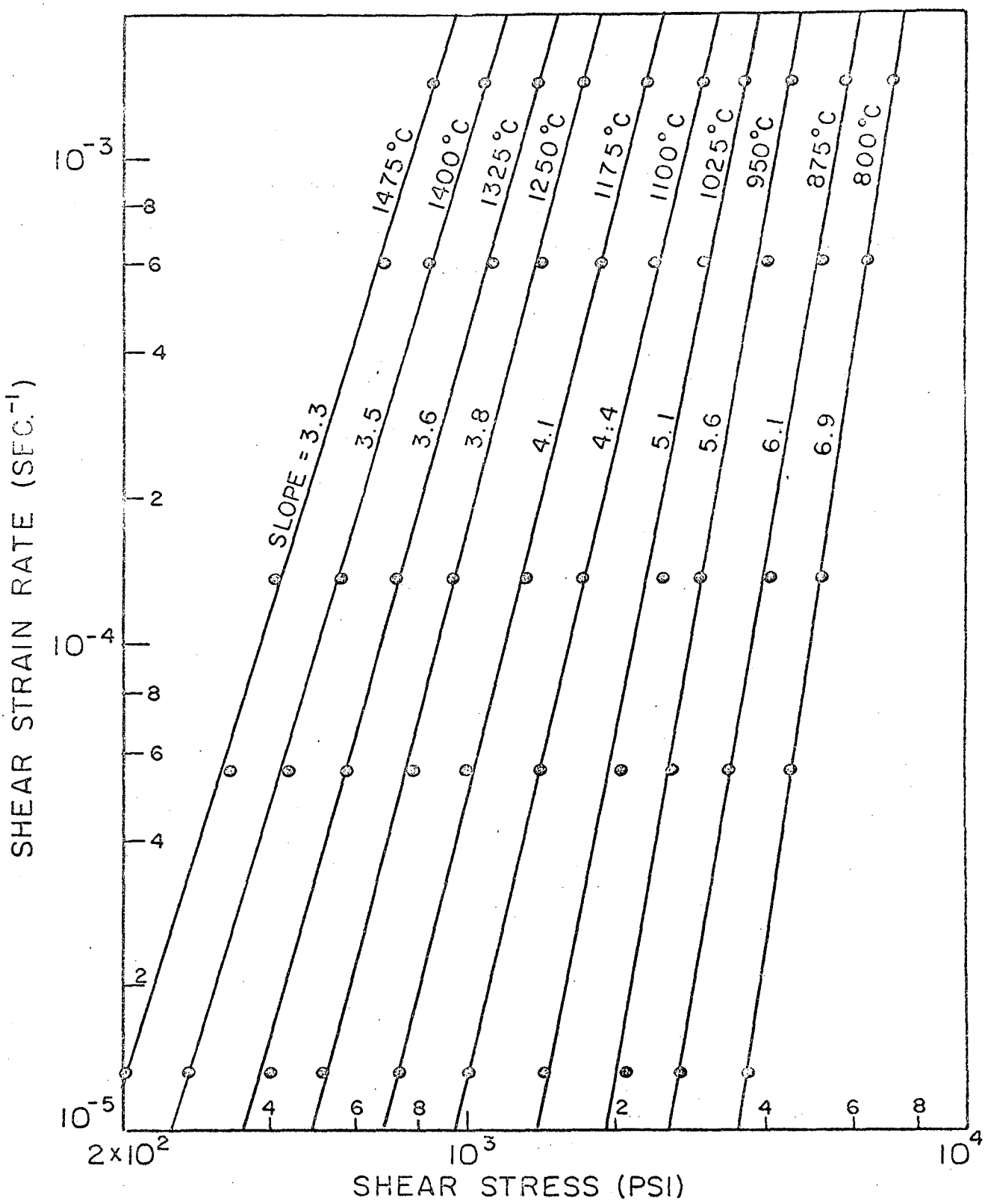

FIG. 4 EFFECT OF STRESS ON THE STRAIN RATE FOR 49.6 AT. % NICKEL ALLOY.

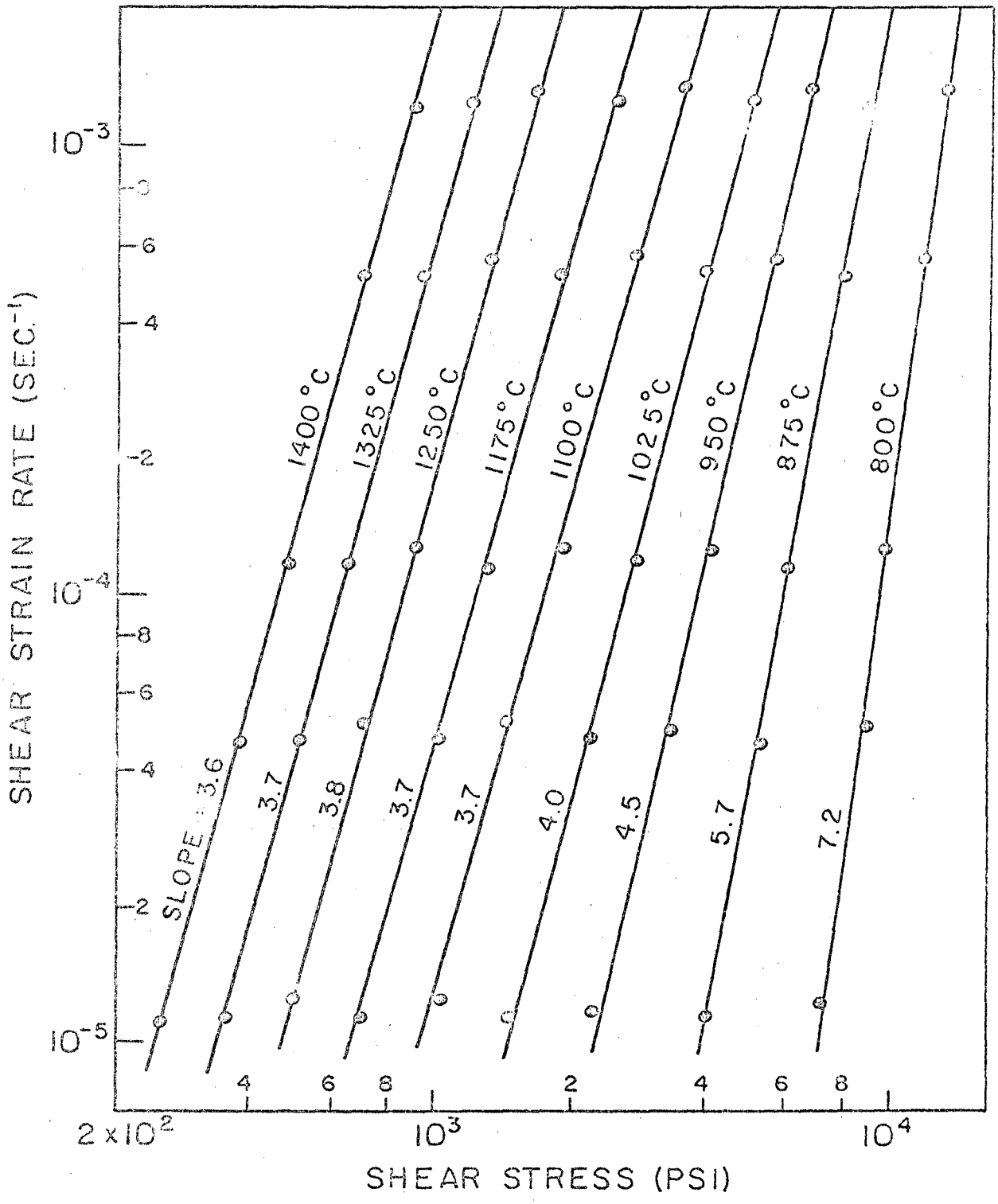

FIG. 5 EFFECT OF STRESS ON THE STRAIN RATE FOR 56.0 AT. % NICKEL ALLOY.

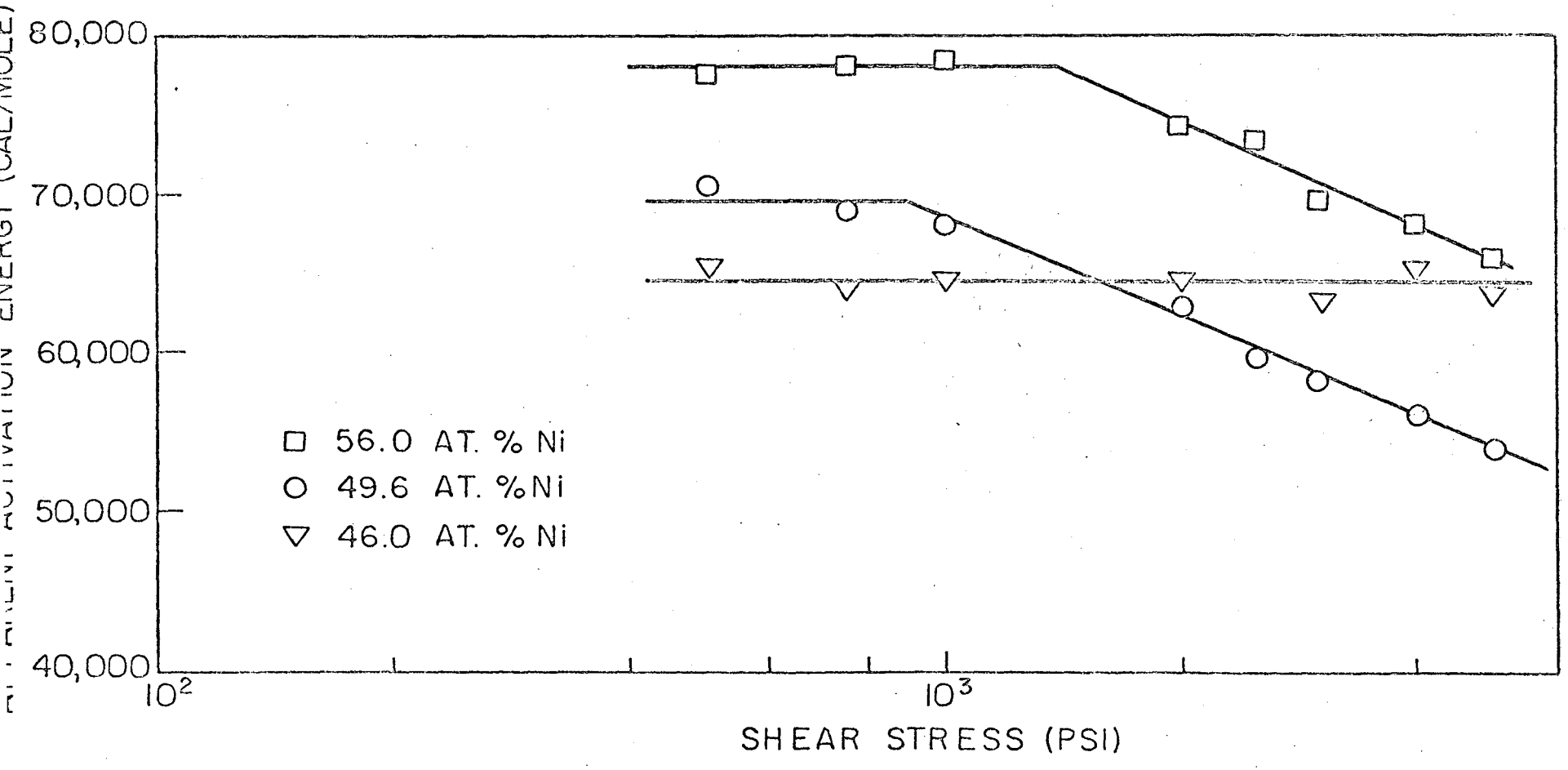

FIG. 6 APPARENT ACTIVATION ENERGIES FOR CREEP.

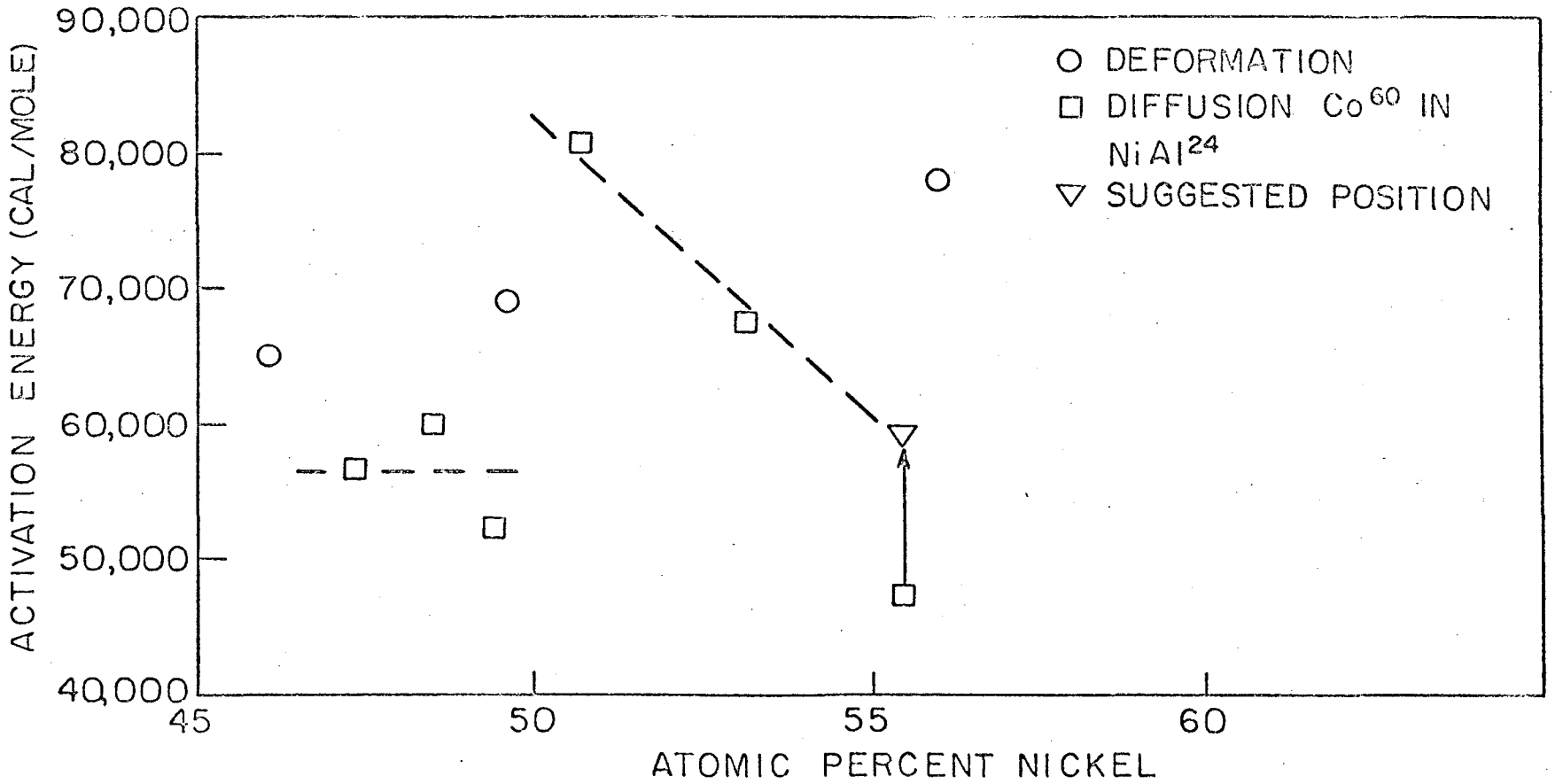

FIG. 7 ACTIVATION ENERGY VERSUS COMPOSITION FOR NiAl ALLOYS.

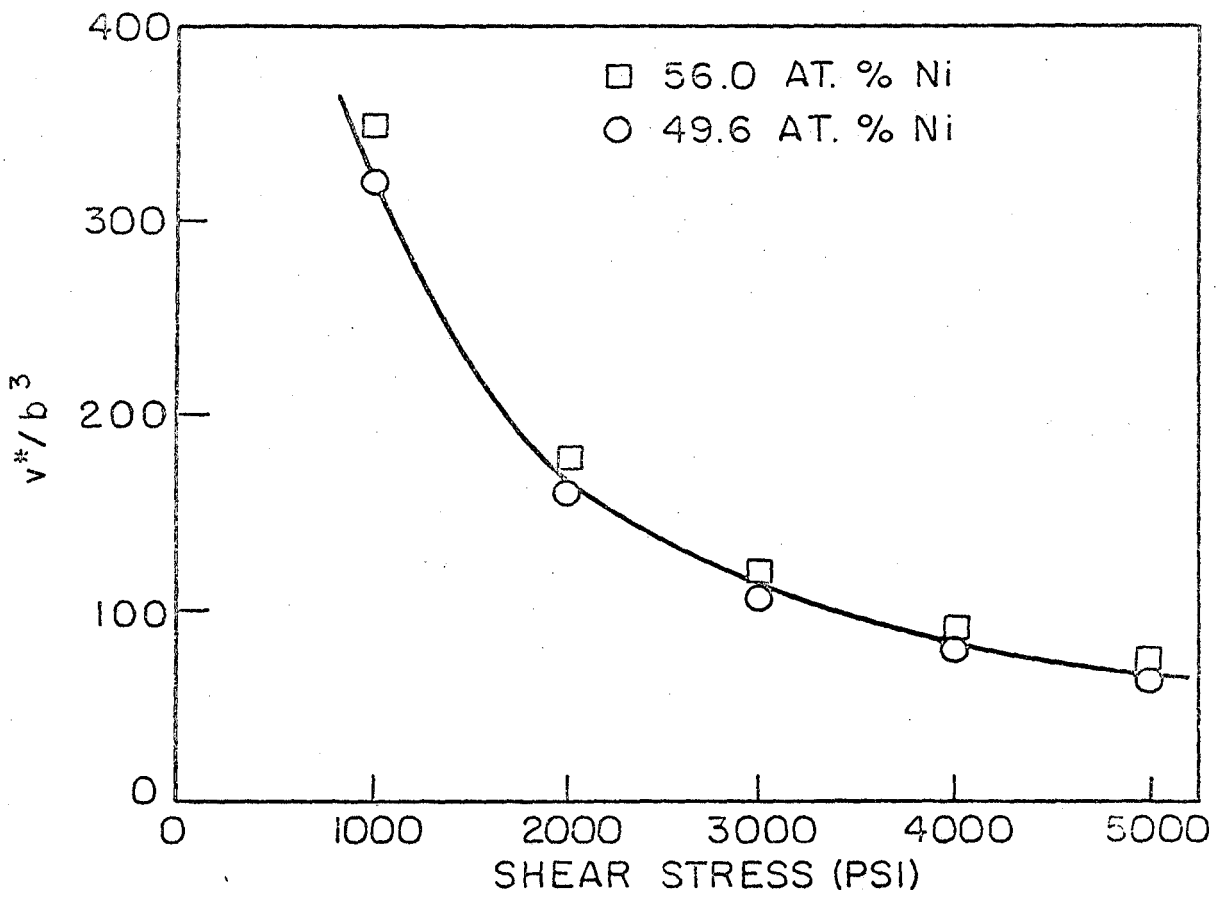

FIG. 8 THE EFFECT OF STRESS ON THE ACTIVATION VOLUME.

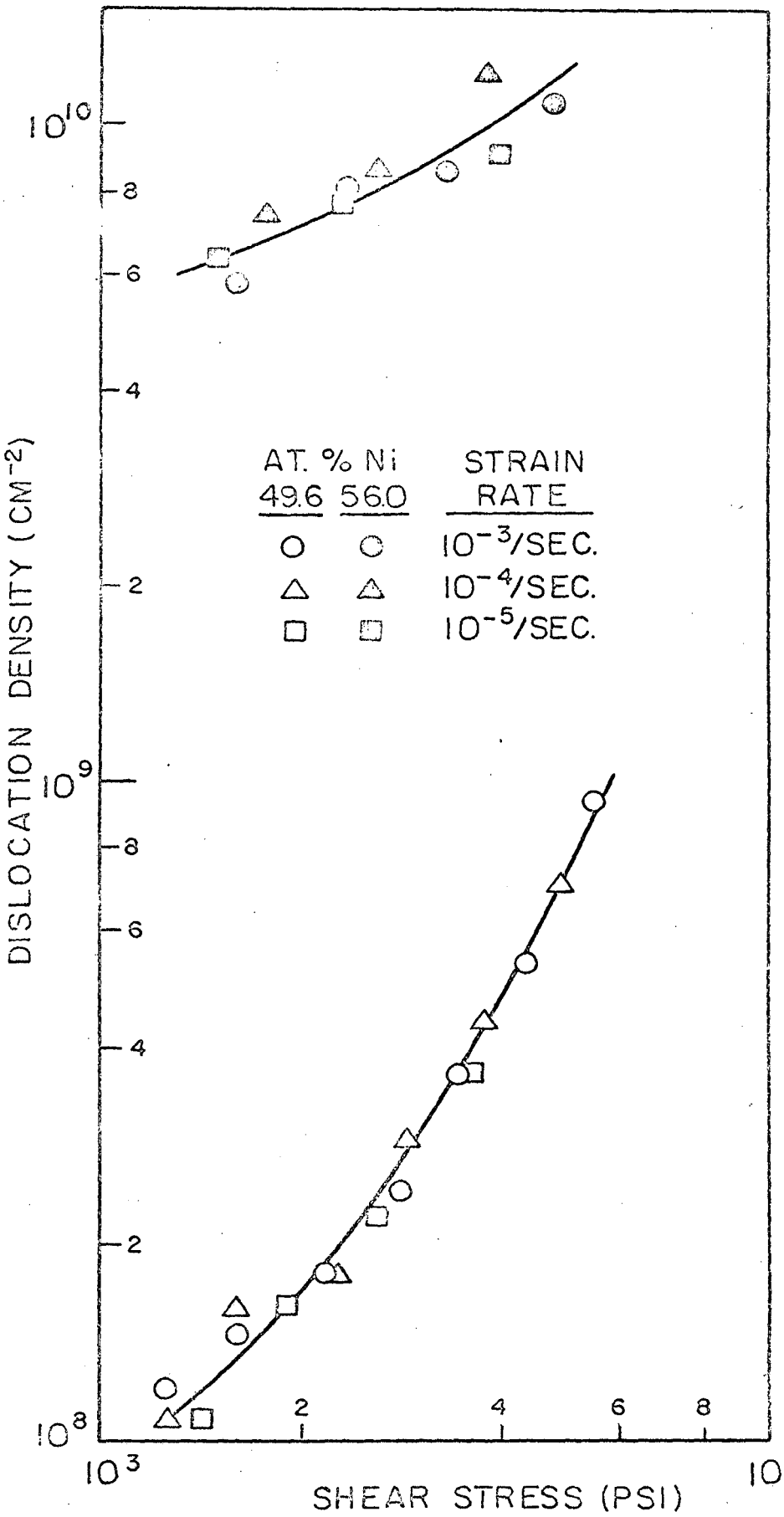

FIG. 9 THE RELATIONSHIP BETWEEN DISLOCATION DENSITY AND FLOW STRESS DURING CREEP.

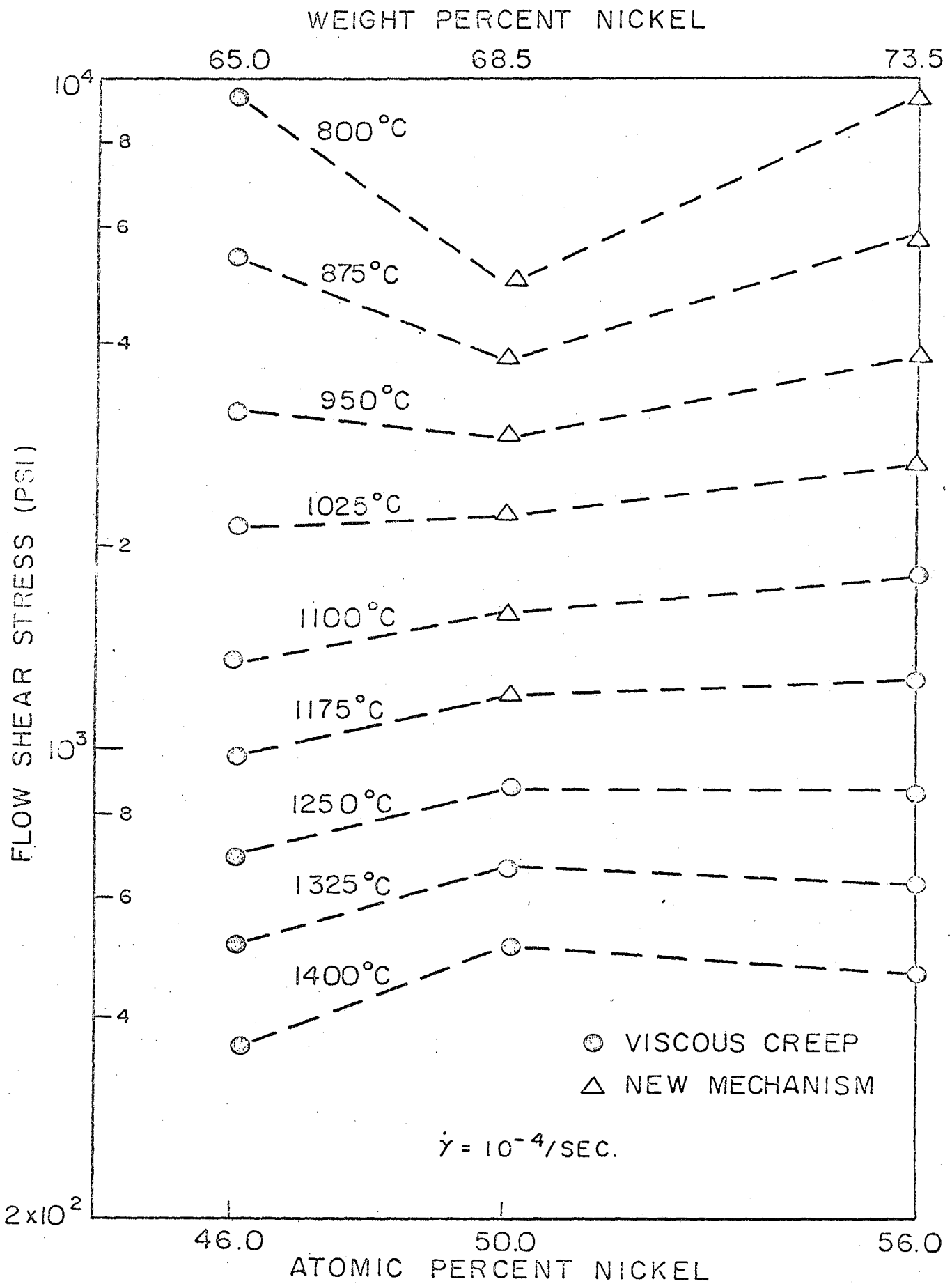

FIG. 10 THE DEPENDENCE OF FLOW STRESS ON COMPOSITION AT CONSTANT TEMPERATURE.